

Evolution of a bosonic mode across the superconducting dome in the high- T_c cuprate

$\text{Pr}_{2-x}\text{Ce}_x\text{CuO}_{4-\delta}$

I. Diamant,^{1,*} S. Hacoheh-Gourgy,¹ and Y. Dagan¹

¹*Raymond and Beverly Sackler School of Physics and Astronomy, Tel-Aviv University, Tel Aviv, 69978, Israel*

(Dated: July 9, 2018)

We report a detailed spectroscopic study of the electron doped cuprate superconductor $\text{Pr}_{2-x}\text{Ce}_x\text{CuO}_{4-\delta}$ using point contact junctions for $x=0.125$ (underdoped), $x=0.15$ (optimally doped) and $x=0.17$ (overdoped). From our conductance measurements we are able to identify bosonic resonances for each doping. These excitations disappear above the critical temperature, and above the critical magnetic field. We find that the energy of the bosonic excitations decreases with doping, which excludes lattice vibrations as the pairing glue. We conclude that the bosonic mediator for these cuprates is more likely to be spin excitations.

PACS numbers: 74.50.+r, 74.62.Dh, 74.72.-h

In the standard theory for superconductivity by Bardeen, Cooper and Schrieffer [1] electrons pair and condense with a characteristic energy scale Δ . This scale manifests itself as a gap in the density of states which can be probed by tunneling spectroscopy.[2] The pairing between electrons occurs despite the coulomb repulsion through a bosonic mediator - "the glue". In their hallmark work McMillan and Rowell[3] showed that for strong enough electron-phonon coupling the tunneling spectra should deviate from the simple BCS density of states. In their work they studied the Lead phonon spectrum and unequivocally established them as the pairing glue in the conventional BCS[1] superconductors.

Electron pairing also occurs in the high temperature cuprate superconductors.[4]. A common characteristic to all these superconductors is the strong dependence of their electronic properties on the number of charge carriers put into the cooper oxygen planes (doping). These charge carriers can be either holes (p-doped) or electrons (n-doped). Many experiments focused on the hole-doped cuprates, while the electron-doped ones remained less studied. Despite many years of research, both on the hole and electron doped side of the phase diagram, there is still a question mark on the nature of the pairing glue. Several theoretical possibilities were suggested: pairing by magnetic interactions,[5–8] phonons [9], and pairing without a glue.[10]

A number of experiments found evidence for bosonic modes in the hole-doped cuprates. However, they could not come to an agreement on the nature of the pairing boson. Pairing by lattice vibrations was suggested by some of them [11–13] while others were interpreted in terms of pairing by spin resonances.[14–16]

On the electron doped side of the phase diagram it has been recently reported that bosonic modes can be found in optimally doped $\text{Pr}_{0.88}\text{LaCe}_{0.12}\text{CuO}_4$ (PLCCO). [17] The deduced energy scale is found to be consistent with both acoustic phonons and spin excitations.

Neutron scattering experiments on optimally doped PLCCO were able to associate a magnetic resonance to

superconductivity and to scale the resonance energy with the critical temperature by: $E_r \approx 5.8k_B T_c$, as was found for other hole-doped cuprates.[18]

Here we show that using point spectroscopy on the n-doped cuprate $\text{Pr}_{2-x}\text{Ce}_x\text{CuO}_{4-\delta}$ (PCCO) we are able to identify bosonic modes and follow their doping dependence both on the overdoped and the underdoped sides of the phase diagram. From this dependence we conclude that the bosons responsible for the pairing interaction in the electron-doped cuprates are most probably spin excitations.

We used pulsed laser deposition to fabricate thin films of the electron-doped cuprate superconductor $\text{Pr}_{2-x}\text{Ce}_x\text{CuO}_{4-\delta}$. Three doping levels were studied: $x=0.125$ (underdoped), $x=0.15$ (optimally doped), and $x=0.17$ (overdoped). The sample was approached by a micro edge Pt-Ir alloy tip using a point contact probe with a 15nm step size. This setup enabled us to vary the height of the potential barrier by changing the sample-tip distance. The distance was varied until clear superconducting features were seen.

In figure 1 we present the typical conductance characteristics for the three doping levels studied at low temperatures. The superconducting energy gap Δ is determined by the energy at which the coherence peaks are observed at low temperatures. The obtained values are consistent with previous measurements.[19] Additional features appear at energies higher than Δ .

To accurately determine the bias at which the high energy features appear, and to understand their origin, we plot the derivative of the conductance as a function of voltage (figure 2). The energy of the features are determined from the position of the step down in the conductance spectra, which manifests itself as a dip in the second derivative for positive biases.[3, 20] A dip in the positive bias side will appear as a peak in the negative bias side and vice versa. We ignore features that do not follow this behavior. Features strictly related to superconductivity will disappear above the critical temperature and critical magnetic field. We were able to verify

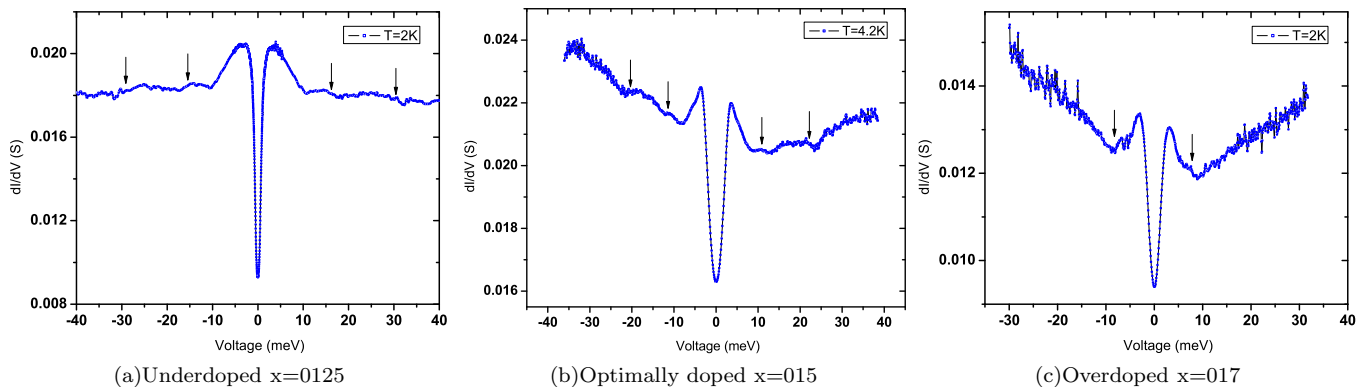


FIG. 1: (Color online) The differential conductance as a function of the applied bias at low temperature. We present three doping levels: (a) the extremely underdoped $x = 0.125$ sample: J0105, (b) the optimally doped $x = 0.15$ Sample: J0803, and (c) the overdoped $x = 0.17$ sample: J0224. The superconducting energy gap Δ is determined by the location of the coherence peaks. The obtained values are consistent with previous measurements.[19] Additional features appear at energies higher than Δ . These features are absent above the critical temperatures, and above the critical magnetic field. The parameters of each junction are: For extremely underdoped sample $x = 0.125$ (a) the gap amplitude is $\Delta = 2.3 \pm 0.3 \text{ meV}$, and the critical temperature at the junction is $T_c = 10.5 \pm 1 \text{ K}$. For optimally doped sample $x = 0.15$ (b): $\Delta = 3.3 \pm 0.2 \text{ meV}$, $T_c(\text{film}) = 16.3 \pm 2 \text{ K}$. And for overdoped sample $x = 0.17$ (c): $\Delta = 2.5 \pm 0.3 \text{ meV}$, $T_c = 12.5 \pm 0.3 \text{ K}$.

this on one sample for each doping.

Below we explain how we differentiated the high energy features from noise and other junction related spurious effects. First, we made sure that these features do not arise from the contact itself. We repeated the measurements for $x = 0.15$ and $x = 0.17$ to make sure that the results are junction and film independent. Second, it is possible that geometrical bound states in the film manifest themselves as a resonance in the conductance spectra.[21]. We measured the optimally doped sample at different thickness and found that the high energy features are thickness independent in contrast with the expected bound state energy. The third possibility is inelastic phonon assisted tunneling.[22, 23] For this case a similar step in the conductance is expected at the phonon energy. The high energy features discussed here are not due to boson assisted tunneling for the following reasons: They disappear below the critical magnetic field and the critical temperature. While for the inelastic case one does not expect such strong field and temperature dependencies. In addition, the case of phonon assisted tunneling is unlikely due to the strong doping dependence discussed below. Last, an additional very large dip feature appears in the d^2I/dV^2 before the first dip we identify as a bosonic mode. This feature is not related to the bosonic modes for the following reasons. The feature appears due to the conductance drop from the coherence peak and does not appear as a step down in the dI/dV spectra. In Addition, it does not have a second harmonic (as explained below). Finally, The feature's energy varies between samples of the same doping level.

We can therefore relate these high energy features to bosonic excitations appearing in the conductance spec-

tra through the frequency dependence of superconducting energy gap $\Delta(\omega)$. Following the logic of Rowell and McMillan we expect the bosonic energy to be shifted by the amplitude of the energy gap. We can therefore define the excitation energy as $\Omega_{1,2} = E_{r_{1,2}} - \Delta$, where $E_{r_{1,2}}$ is the energy of the high energy feature taken from the data, Δ is the amplitude of the energy gap, and $\Omega_{1,2}$ is the bosonic resonance energy.

In figure 2 we present the differential conductance derivative focusing on the low bias region. In this region the superconducting gap as well as the bosonic features appear. While Δ clearly appears in the differential conductance, the bosonic features are conspicuous in the conductance derivative. For phonons, Morrel and Anderson showed, using the Einstein approximation, that the gap parameter $\Delta(\omega)$ exhibits features at the phonon frequency and its multiplications: $\omega_L, 2\omega_L, \dots$ with ω_L a longitudinal phonon frequency.[24]. Similar results were obtained by Swihart [25] and Culler [26] using a Debye approximation. These theoretical findings were also confirmed experimentally.[27] This pattern also appears in our data: $\Omega_2 = 2\Omega_1$. This strengthens the identification of these features as bosonic modes related to superconductivity.

In view of the above we made the following steps in order to find the energy of the bosonic mode for each doping level: First, we found the energy of the dip (peak) in the positive (negative) bias and the error as the full width half maximum for the first and second harmonic. We then averaged the positive and negative bias, $\Omega = \frac{1}{2}(\Omega_1 + \Omega_2/2)$, as well as the error. This procedure was carried out for each sample and each junction.

In figure 3 we plot the energy of the bosonic mode, Ω ,

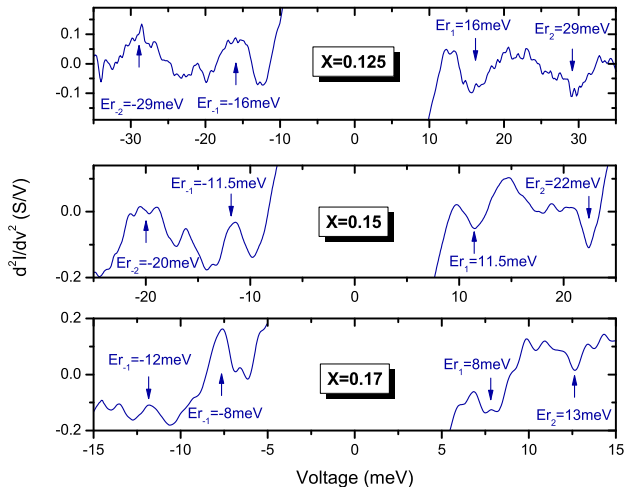


FIG. 2: (Color online) The derivative of the differential conductance (d^2I/dV^2) as a function of the applied bias for the three different doping levels appearing in figure 1: (a) the extremely underdoped $x = 0.125$ J0105, (b) the optimally doped $x = 0.15$ J0803, and (c) the overdoped $x = 0.17$ J0224. For each sample we note the energy at which the bosonic mode appear.

as a function of doping. We note that the gap amplitude in our measurements follows the critical temperature behavior as a function of doping as reported elsewhere.[19] From our analysis we find that Ω strongly decreases with increasing doping. For the doping range studied, the amount of cerium substitution changes by merely 1%. We therefore do not expect such a strong variation of lattice vibration frequency by such a minute change. Despite the above, a doping driven structural phase transition can manifest itself in an abrupt change in the phonon spectrum. Such a transition, however, is not observed for PCCO in this doping regime.[28, 29]

We draw a linear fit of the excitation energy as a function of the doping, and find that the energy extrapolates to zero at approximately $x = 0.2$. We are not aware of a theoretical prediction for the doping dependence of the bosonic mode. The fact that the line extrapolates to zero right at the edge of the superconducting dome is intriguing.

We summarize our experimental observations. We observed resonances in the point contact spectra appearing in $\Omega + \Delta$, and $2\Omega + \Delta$. These features disappear above the critical temperature, and above the critical magnetic field. We relate them to bosonic excitations responsible for superconductivity. We find that these bosonic excitations are doping dependent.

We shall now discuss our results in the context of other experiments and predictions. Clear tunneling features were observed in previous planar tunneling experiments [19, 30], however, these measurements did not exhibit conspicuous signatures of bosonic structures in

the conductance spectra. A possible explanation for this could arise from the large contact size used relative to the coherence length, ξ . This can be understood noting that STM measurements on the hole-doped $\text{Bi}_2\text{Sr}_2\text{CaCu}_2\text{O}_{8-\delta}$ showed large spatial variation in the gap amplitude over a length scale of the order of ξ . [12, 31] For the electron-doped cuprates ξ is ten times larger than for $\text{Bi}_2\text{Sr}_2\text{CaCu}_2\text{O}_{8-\delta}$, [32] yet, it is much smaller comparing to the large scale of the planar junctions. Since the bosonic excitation is shifted by the value of the gap, [33] and since tunneling in this large scale contact is actually a measurement of an averaged gap amplitudes, the bosonic excitation energy is smeared on the energy axis. In contrast, the junction size in point contact measurements is much smaller. It is of the order of the coherence length of PCCO. It is therefore possible that this point contact junction size is sufficient to obtain a relatively constant gap amplitude and consequently to enable the observation of bosonic modes.

We compare our result to the phenomenological relation $\Omega = 5.8k_B T_c$ drawn from neutron scattering experiments.[18] For the optimally doped sample we get $\Omega = 8.2\text{meV}$, which falls within the error bar of our results. For the overdoped sample this relation falls slightly above our data point. However, the underdoped sample deviates from this relation. We speculate that this difference stems from the extent of the antiferromagnetic region in the n-doped cuprates compare to the p-doped ones.

Finally, Niestemski *et al.*[17] analyzed STM data to identify bosonic excitations in optimally doped PLCCO. However, Guo-meng Zhao [20] noted, based on the analysis of McMillan and Rowell [3], that the bosonic energy should be identified as a step down in the conductance which yields a dip in the second derivative for positive biases. This prediction also appears in the theoretical work by Ar. Abanov and A. V. Chubukov [34], in their work they also predict that the bosonic energy, Ω , should be smaller than twice the energy gap. This is in contrast to our data.

In summary, we observed structures in the derivative of the conductance characteristics. We eliminate boson assisted tunneling, spurious noise and geometrical effects, as possible explanations for these features. The temperature, field and voltage dependencies of these features suggest that they arise from bosonic modes reflected through the energy dependence of the superconducting gap. Pairing by both phonons and magnetic excitations predicts a step down feature in the tunneling spectra. However, the doping dependence of the boson energy casts strong doubts on phonon mediated superconductivity in the electron-doped cuprates. Our results are therefore more in line with the spin excitation pairing theory.

We thank A. Yechzkel for machining the differential screw. This research was partially supported by the Binational Science Foundation grant number 2006385, and

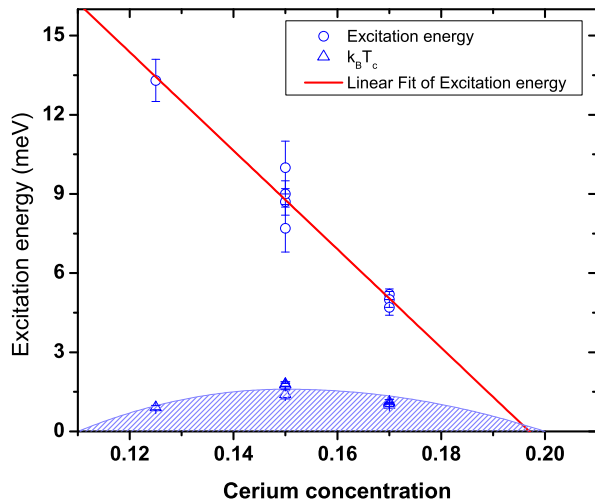


FIG. 3: (Color online) The spin excitation energy (\circ) and the critical temperature (\triangle) (The dome is outlined as a guide to the eye) as a function of doping. Each symbol corresponds to a different junction (The error bars reflect the averaged width of both features). We note that the gap amplitude in our measurements follows the critical temperature behavior as a function of doping as reported elsewhere.[19] From our analysis we find that Ω strongly decreases with increasing doping. We draw a linear fit of the excitation energy as a function of the doping, and find that the energy extrapolates to zero at $x = 0.2$, which is just beyond the superconducting dome.

the Israel Science Foundation grant number 1421/08.

* diamanti@post.tau.ac.il

- [1] J. Bardeen, L. N. Cooper, and J. R. Schrieffer, Phys. Rev. **108**, 1175 (1957).
 [2] I. Giaever and K. Megerle, Phys. Rev. **122**, 1101 (1961).
 [3] W. L. McMillan and J. M. Rowell, Phys. Rev. Lett. **14**, 108 (1965).
 [4] C. E. Gough, M. S. Colclough, E. M. Forgan, R. G. Jordan, M. Keene, C. M. Muirhead, A. I. M. Rae, N. Thomas, J. S. Abell, and S. Sutton, Nature **326**, 855 (1987).
 [5] P. Monthoux and D. J. Scalapino, Phys. Rev. Lett. **72**, 1874 (1994).
 [6] P. Monthoux and D. Pines, Phys. Rev. Lett. **69**, 961 (1992).
 [7] A. Chubukov, *Superconductivity: Novel superconductors* (Springer, 2008), p. 1349.
 [8] D. Manske, I. Eremin, and K. H. Bennemann, Phys. Rev. B **62**, 13922 (2000).

- [9] J. Song and J. F. Annett, Phys. Rev. B **51**, 3840 (1995).
 [10] P. W. Anderson, Science **317**, 1705 (2007).
 [11] A. Lanzara, P. V. Bogdanov, X. J. Zhou, S. A. Kellar, D. L. Feng, E. D. Lu, T. Yoshida, H. Eisaki, A. Fujimori, K. Kishio, et al., Nature **412**, 510 (2001).
 [12] J. Lee, K. Fujita, K. McElroy, J. A. Slezak, M. Wang, Y. Aiura, H. Bando, M. Ishikado, T. Masui, J.-X. Zhu, et al., Nature **442**, 546 (2006).
 [13] R. J. McQueeney, Y. Petrov, T. Egami, M. Yethiraj, G. Shirane, and Y. Endoh, Phys. Rev. Lett. **82**, 628 (1999).
 [14] N. Jenkins, Y. Fasano, C. Berthod, I. Maggio-Aprile, A. Piriou, E. Giannini, B. W. Hoogenboom, C. Hess, T. Cren, and O. Fischer, Phys. Rev. Lett. **103**, 227001 (2009).
 [15] M. R. Norman, H. Ding, J. C. Campuzano, T. Takeuchi, M. Randeria, T. Yokoya, T. Takahashi, T. Mochiku, and K. Kadowaki, Phys. Rev. Lett. **79**, 3506 (1997).
 [16] Rossat-Mignod, L. P. Regnault, P. Bourges, C. Vettier, P. Burlet, and J. Y. Henry, Physica C **185**, 86 (1991).
 [17] F. C. Niestemski, S. Kunwar, S. Zhou, S. Li, H. Ding, Z. Wang, P. Dai, and V. Madhavan, Nature **450**, 1058 (2007).
 [18] S. Wilson, P. Dai, S. Li, S. Chi, H. J. Kang, and J. W. Lynn, Nature **442**, 59 (2006).
 [19] I. Diamant, R. L. Greene, and Y. Dagan, Physical Review B **80**, 012508 (2009).
 [20] G.-m. Zhao, Phys. Rev. Lett. **103**, 236403 (2009).
 [21] C. Nguyen, H. Kroemer, and E. L. Hu, Phys. Rev. Lett. **69**, 2847 (1992).
 [22] J. R. Kirtley, Phys. Rev. B **47**, 11379 (1993).
 [23] W. Franz, *Tunneling Phenomena in Solids* (Plenum Press, New York, 1969), p. 207.
 [24] P. Morel and P. W. Anderson, Phys. Rev. **125**, 1263 (1962).
 [25] J. Swihart, IBM J. Res. Develop. **6**, 14 (1962).
 [26] G. J. Culler, B. D. Fried, R. W. Huff, and J. R. Schrieffer, Phys. Rev. Lett. **8**, 399 (1962).
 [27] I. Giaever, H. R. Hart, and K. Megerle, Phys. Rev. **126**, 941 (1962).
 [28] N. Armitage, P. Fournier, and R. Greene, arXiv:0906.2931 (2009).
 [29] J.-M. Tarascon, E. Wang, L. H. Greene, B. G. Bagley, G. W. Hull, S. M. D'Egidio, P. F. Miceli, Z. Z. Wang, T. W. Jing, J. Clayhold, et al., Phys. Rev. B **40**, 4494 (1989).
 [30] Y. Dagan, R. Beck, and R. L. Greene, Phys. Rev. Lett. **99**, 147004 (2007).
 [31] K. M. Lang, V. Madhavan, J. E. Hoffman, E. W. Hudson, H. Eisaki, S. Uchida, and J. Davis, Nature **415**, 412 (2002).
 [32] C. Howald, P. Fournier, and A. Kapitulnik, Phys. Rev. B **64**, 100504 (2001).
 [33] W. A. Harrison, Phys. Rev. **123**, 85 (1961).
 [34] A. Abanov and A. V. Chubukov, Phys. Rev. B **61**, R9241 (2000).